

Interferometric Mapping of Magnetic Fields: G30.79 FIR 10

P. Cortes

Astronomy Department, University of Illinois at Urbana-Champaign, IL 61801

R. M. Crutcher

Astronomy Department, University of Illinois at Urbana-Champaign, IL 61801

ABSTRACT

We present polarization maps of G30.79 FIR 10 (in W43) from thermal dust emission at 1.3 mm and from CO J=2 \rightarrow 1 line emission. The observations were obtained using the Berkeley-Illinois-Maryland Association array in the period 2002-2004. The G30.79 FIR 10 region shows an ordered polarization pattern in dust emission, which suggests an hourglass shape for the magnetic field. Only marginal detections for line polarization were made from this region. Application of the Chandrasekhar-Fermi method yielded $B_{pos} \approx 1.7$ mG and a statistically corrected mass to magnetic flux ratio $\lambda_C \approx 0.9$, or essentially critical.

Subject headings: ISM: magnetic fields ISM:polarization stars: formation

1. Introduction

The star formation process involves a number of physical parameters, of which the magnetic field is the least observed. Magnetic field observations are divided into measurements of the Zeeman effect (in order to obtain the magnetic field strength in the line of sight), and linear polarization observations of dust and spectral-line emission. Polarization of dust emission is believed to be perpendicular to the magnetic field under most conditions (Lazarian 2003); hence, polarization of dust emission has been used as a major probe for the magnetic field geometry. In order to efficiently map the polarization of dust emission and infer information about the magnetic field morphology, high resolution observations are required. The BIMA millimeter interferometer has been used previously to obtain high-resolution polarization maps in several star forming cores (Rao et al. 1998; Girart et al. 1999; Lai 1999; Lai et al. 2002, 2003). These results show fairly uniform polarization morphologies over the main continuum sources, suggesting that magnetic fields are strong, and therefore cannot be ignored by star formation theory. However, the number of star formation regions with maps of magnetic fields remains small, and every new result is significant.

Spectral line linear polarization has been suggested to arise from molecular clouds under anisotropy conditions (Goldreich & Kylafis 1981). The prediction suggests that a few percent of linearly polarized radiation should be detected from molecular clouds and circumstellar envelopes in the presence of a magnetic field. It is also predicted that the molecular line polarization will be either parallel or perpendicular to the magnetic field, depending on the angles between the line of sight, the magnetic field, and the anisotropic excitation direction (Goldreich & Kylafis 1982). This process is known as the Goldreich - Kylafis effect.

In order to use these techniques, we mapped the massive star forming region G30.79 FIR 10 with the BIMA array. We measured continuum polarization at 1.3 mm and CO $J = 2 \rightarrow 1$ line polarization obtaining high resolution interferometric maps for both measurements.

The remainder of this paper is divided in five major sections. Section 2 reviews information about the source, section 3 describes the observation procedure. Section 4 presents the results, section 5 gives the discussion, and section 6 the conclusions and summary.

2. Source Description

G30.79 is a large dust continuum source located within the W 43 region, which is an H II region-molecular cloud complex near $l = 31^\circ, b = 0^\circ$. We observed G30.79 FIR 10, which is a massive and dense component in the G30.79 complex. Liszt (1995) observed G30.79 in HCO⁺ and ¹³CO, concluding that the presence of several rings and shells in the dense molecular gas was a disturbance product of star formation. Vallée & Bastien (2000) observed the dust continuum emission in this source at 760 μm with the JCMT telescope. They found linear polarization of about 1.9% with a position angle (P.A.) of 160° at FIR 10. Mooney et al. (1995) also observed this source at 1.3 mm using the IRAM 30-meter antenna, detecting a total flux of 13.6 Jy; their wide field map shows FIR 10 and the extended H II region in the G30.79 complex. H₂O masers have also been observed toward this region (Cesaroni et al. 1988) that are within a half arcsecond of the peak in the Mooney et al. (1995) map and might be a signature of massive star formation. No centimeter radio-continuum emission seems to be associated with FIR 10, which suggests that the source is in an early stage of evolution. Motte et al. (2003) mapped the W43 main complex in dust continuum emission at 1.3 mm and 350 μm with the IRAM 30-m telescope and the CSO, respectively. They also mapped the HCO⁺ $J = 3 \rightarrow 2$ line and measured H¹³CO⁺ $J = 3 \rightarrow 2$ towards prominent dust maxima. One of the maxima, W43-MM1, is the compact fragment we mapped with BIMA. Motte et al. (2003) found $v_{lsr} = 98.8 \text{ km s}^{-1}$, $\Delta v = 5.9 \text{ km s}^{-1}$ (from H¹³CO⁺), $T_{\text{dust}} \sim 19 \text{ K}$, $M \sim 3600 M_{\odot}$, and $n(\text{H}_2) \sim 8.8 \times 10^6 \text{ cm}^{-3}$. They estimated the virial mass to be $M_{\text{vir}} \sim 1000 M_{\odot}$, suggesting that this compact fragment should be in a state

of gravitational collapse unless there are other sources of support than kinetic energy. The W43 region, is therefore, an excellent region for the study of the earliest stages of massive star formation.

3. Observation Procedure

We observed G30.79 FIR 10 between October 2002 to May 2004, mapping the continuum emission at 1.3 mm and the CO $J = 2 \rightarrow 1$ molecular line (at 230 GHz); four tracks with the BIMA array in C configuration were obtained. We set the digital correlator in mode 8 to observe both the continuum and the CO $J = 2 \rightarrow 1$ line simultaneously. The 750 MHz lower side band was combined with 700 MHz from the upper side band to map the continuum emission, leaving a 50 MHz window for the CO line observation (at a resolution of 1.02 km s^{-1}). Each BIMA telescope has a single receiver, and thus the two polarizations were observed sequentially. A quarter wave plate to select either right (R) or left (L) circular polarization was alternately switched into the signal path ahead of the receiver. Switching between polarizations was sufficiently rapid (every 11.5 seconds) to give essentially identical uv-coverage. Cross-correlating the R and L circularly polarized signals from the sky gave RR, LL, LR, and RL for each interferometer baseline, from which maps in the four Stokes parameters were produced. The source 1743-038 was used as phase calibrator for G30.79 FIR 10. The instrumental polarization was calibrated by observing 3C279, and the “leakages” solutions were calculated from this observation. We used the same calibration procedure described by Lai (1999).

The Stokes images I, U, Q and V were obtained by Fourier transforming the visibility data using natural weighting. The MIRIAD (Sault et al. 1995) package was used for data reduction. G30.79 FIR 10 is close to the equator; therefore, we expect strong sidelobes in the beam pattern. We followed Chernin & Welch (1995), who observed NGC2071IR (also a source close to the equator) with the BIMA array, and imaged only out to $20''$ radius, due to the strong sidelobes.

4. Observational Results

4.1. 1.3 mm Continuum

Polarized dust emission was detected and mapped toward G30.79 FIR 10 (Figure 1) with a beam size of $5.6'' \times 3.6''$ and a beam P.A. of 4.3° . The Stokes I map shows a peak emission of 1.6 Jy beam^{-1} ; this peak is consistent with Mooney et al. (1995) observations at

the same wavelength. Most of the emission in Figure 1 comes from a compact core $\sim 8''$ in radius.

The polarized emission shown in Figure 1 has a 3σ level of significance, a peak polarized intensity of $0.03 \text{ Jy beam}^{-1}$, and a mean position angle of $4.6^\circ \pm 6.1^\circ$. The polarization direction is different in the northern and southern regions; the mean P.A. in the north is $-33.2^\circ \pm 6.6^\circ$, and in the south is $23.9^\circ \pm 5.5^\circ$. The polarization is fairly uniform in fractional polarization and smooth in its direction change from north to south, (see Table 1). Vallée & Bastien (2000) observed G30.79 FIR 10 using the JCMT telescope at $760 \mu\text{m}$. They detected continuum polarization at two points in FIR 10. Only one of them is in the general area of our map; however, this point is $\sim 15''$ south of the center of our polarization pattern. Hence, these results cannot be compared directly with ours.

4.2. CO $J = 2 \rightarrow 1$

Polarized emission from the CO $J = 2 \rightarrow 1$ was detected (Figure 2). The Stokes I map shows three CO peaks which cover a similar area as the continuum emission. Our peak emission is 1.4 Jy beam^{-1} with a beam size of $5.5'' \times 3.5''$ and a beam P.A. of 4.0° . We only detected a level of polarized emission of at least 3σ at three independent positions in the core. These three points show two distinctive directions which appear to be orthogonal to each other. The polarization in the southern part of the map shows a mean P.A. of $25.5^\circ \pm 4.4^\circ$, while the north-western part of the core shows a mean P.A. of $-31.7^\circ \pm 4.5^\circ$. Line polarized emission appears to be parallel to dust polarized emission over the same area in the south; the average P.A. difference is $\sim 2^\circ$ which suggests that the magnetic field is perpendicular to the polarization. However, in the north-western region the average difference in P.A. is $\sim 54^\circ$. It is possible that our interferometric observations are resolving out the CO emission, which will make the fractional polarization measurements unreliable.

5. Discussion

We mapped polarized dust emission at 1.3 mm from G30.79 FIR 10, and Vallée & Bastien (2000) detected polarized dust emission at $760 \mu\text{m}$. The emission at both wavelengths seem to be dominated by dust, which is reinforced by the lack of centimeter radio continuum emission from this source. A fully developed H II region is present in the G30.79 region, but its ionization front has not yet reached FIR 10; the H II region appears to be $\sim 2 \text{ pc}$ away from the FIR 10 source (Mooney et al. 1995). Water masers have also been observed, which

is a signpost for high mass star formation. Based on this evidence, we believe that G30.79 FIR 10 is in an early stage of evolution.

We inferred the source parameters from our data using an area $\theta_s = 20'' \times 20''$, which corresponds to the area over which we mapped the polarized flux of the core. The dust absorption cross section per H-atom is approximated by a power law (Mezger et al. 1990)

$$\tau_\lambda = N_{\text{H}}\sigma_\lambda^{\text{H}} = N_{\text{H}}(Z/Z_\odot)b(7 \times 10^{-21}\lambda^{-2}), \quad (1)$$

where λ is the wavelength, $N_{\text{H}} = N(\text{H}) + 2N(\text{H}_2)$ is the total hydrogen column density, Z/Z_\odot the relative metallicity, and b is a parameter which reflects the variation of dust absorption cross sections (Mezger et al. 1990). Two values are used for b ; $b = 1.9$ reproduces estimates of $\sigma_{400\mu\text{m}} \sim 8.3 \times 10^{-26} \text{ cm}^2(\text{H-atom})^{-1}$, which represents molecular gas of moderate density $n(\text{H}_2) < 10^6 \text{ cm}^{-3}$, and $b = 3.4$ relates to dust around deeply embedded IR sources at higher densities. Apparently a value of $b = 3.4$ was used by Mooney et al. (1995) in their estimates on G30.79 FIR 10. We used the expressions for the cloud mass and the column density given by Mooney et al. (1995):

$$(N_{\text{H}}/\text{cm}^{-2}) = 1.93 \times 10^{15} \frac{(S_{\nu,avg}/\text{Jy})\lambda_{\mu\text{m}}^4}{(\theta_s/\text{arcsec})^2(Z/Z_\odot)bT} \frac{e^x - 1}{x} \quad (2)$$

$$(M_{\text{H}}) = 4.1 \times 10^{-10} \frac{(S_{\nu,avg}/\text{Jy})\lambda_{\mu\text{m}}^4 D_{\text{kpc}}^2}{(Z/Z_\odot)bT} \frac{e^x - 1}{x}, \quad (3)$$

where $S_{\nu,avg}$ is the averaged flux from the source, $\theta_s = \sqrt{\theta_{s,min} \times \theta_{s,max}}$ is the angular source size, $x = \frac{1.44 \times 10^4}{\lambda_{\mu\text{m}} T}$ is the $\frac{hc}{\lambda kT}$ factor for the Planck function, and D_{kpc} is the distance to the source in kpc. We obtained $S_{\nu,avg}$ by averaging the continuum emission over an area of $20'' \times 20''$, which gives 4.7 Jy. From their 1.3 mm single dish observations, Mooney et al. (1995) obtained 13.6 Jy for a source of $25.4'' \times 33.2''$. Their larger result is due both to the larger area over which they averaged and to loss of flux in the interferometer data due to missing short uv-spacings. We used $T = 20$ K, the same dust temperature used by Mooney et al. (1995), who noted the uncertainty of the value, which is based on dust models. Motte et al. (2003) also observed G30.79 FIR 10 (which they called W43-MM1); they fitted a gray body model obtaining a dust temperature of 19 K. A distance of 5.5 kpc to G30.79 FIR 10 was used (Motte et al. 2003). From our date, we find $N_{\text{H}} = 1.3 \times 10^{24} \text{ cm}^{-2}$ and $M_{\text{H}} = 3300 M_\odot$. The mass is in agreement with Motte et al. (2003) who estimated $M_{\text{H}} = 3600 M_\odot$. However, this value is lower than the values calculated by Vallée & Bastien (2000), who estimated a mass $M_{\text{H}} = 9 \times 10^3 M_\odot$, and Mooney et al. (1995), who calculated $M_{\text{H}} = 1.1 \times 10^4 M_\odot$. This difference can be explained due to the larger distance assumed by the later investigators.

Assuming magnetic alignment, our polarized dust emission map suggests a poloidal morphology for the magnetic field. This is seen by rotating the line segments in Figure 1 by 90° . This poloidal morphology hints at an hourglass shape for the magnetic field in this core. The proposed field morphology is shown by thick dashed lines Figure 1.

Using the Chandrasekhar-Fermi effect (Chandrasekhar & Fermi 1953), we can estimate the magnetic field strength from the analysis of the small scale randomness of magnetic field lines. We used the expression in Crutcher et al. (2004) to estimate the magnetic field strength:

$$B_{pos} = 9.3 \frac{\sqrt{n(\text{H}_2)} \Delta V}{\delta\phi} \quad (4)$$

where B_{pos} is the magnetic field strength in μG , $n(\text{H}_2)$ is in cm^{-3} , ΔV is the FWHM velocity width in km s^{-1} , and $\delta\phi$ is the P.A. dispersion in degrees.

We used $\Delta V = 5.9 \text{ km s}^{-1}$ from the apparently optically thin H^{13}CO^+ measured with a $29''$ beam (Motte et al. 2003). Our $N_{\text{H}} = 1.3 \times 10^{24} \text{ cm}^{-2}$ implies $N(\text{H}_2) = 6.5 \times 10^{23} \text{ cm}^{-2}$, which gives $n(\text{H}_2) = 4.8 \times 10^5 \text{ cm}^{-3}$ for a core diameter of $16''$ (0.43 pc). The weighted-mean P.A. dispersion $\delta\phi = 21.9^\circ$ (after correction for 4.7° contribution from measurement uncertainties) was calculated from our polarized dust observations. These values yield $B_{pos} = 1.7 \text{ mG}$. Although, this value may seem extraordinarily high, it is similar to field strengths estimated from maser Zeeman splitting at similar gas densities in other clouds.

Using our estimate above for the column density, we can calculate the mass to magnetic flux ratio in term of the critical value (Crutcher 2004):

$$\lambda = 7.6 \times 10^{-21} \frac{N(\text{H}_2)}{B} \quad (5)$$

where $N(\text{H}_2)$ is in cm^{-2} and B in μG . We obtained a value of $\lambda \approx 2.8$, which is slightly supercritical. Applying the statistical geometrical correction factor of $1/3$ (Crutcher 2004), $\lambda_C \approx 0.9$, which is essentially critical.

Our CO $J = 2 \rightarrow 1$ line polarization detections are too scarce to yield any significant information about the magnetic field. However, comparing the CO polarized emission to the dust polarized emission may help in getting information about the sources of anisotropy in this region. Figure 2 shows that at the south-eastern side of the map the CO polarization is parallel to the polarized dust emission, and in the north-western part of the map they may be roughly orthogonal. Previous polarization observations in sources like DR21(OH) showed CO $J = 2 \rightarrow 1$ polarization perpendicular to the polarization of dust emission over the main

sources (Lai et al. 2003). A theoretical study by Cortes et al. (2005) suggested that line polarization traces the magnetic field at lower densities than the dust, and the orientation of the line polarization will depend on the degree of anisotropy in the region. Cortes et al. (2005) concluded that the presence of hot continuum sources will preferentially produce CO $J = 2 \rightarrow 1$ polarization that will be perpendicular to the dust polarization. In the case of G30.79 FIR10 it is difficult to draw any conclusion without CO $J = 1 \rightarrow 0$ polarization data and a detailed modeling of the source.

6. Summary and conclusions

We observed G30.79 FIR 10 and successfully mapped CO $J = 2 \rightarrow 1$ line and 1.3 mm dust continuum polarized emission with a resolution of $4''$.

G30.79 FIR 10 is not a well studied region; however, there is evidence that points toward an early stage of development of high-mass star formation. We found a remarkably uniform pattern in our polarized dust emission map, which suggests an hourglass magnetic field morphology. Using the Chandrasekhar-Fermi method, we inferred a plane-of-the-sky magnetic field strength 1.7 mG, which yielded a geometry-corrected mass to magnetic flux ratio of 0.9 to respect to critical. This result is similar to those found in many other regions of low-mass and high-mass star formation.

Polarized line emission was also detected in this region; these results pose questions about the sources of anisotropy, which will require more detailed modeling.

This research was partially funded by NSF grants AST 02-05810 and 02-28953.

REFERENCES

- Cesaroni, R., Palagi, F., Felli, M., Catarzi, M., Comoretto, G., di Francos, Giovanardi, C., & Palla, F. 1988, *A&AS*, 76, 445
- Chandrasekhar, S., & Fermi, E. 1953, *ApJ*, 118, 113
- Chernin, L. M., & Welch, W. J. 1995, *ApJ*, 440, L21
- Cortes, P. C., Crutcher, R. M., & Watson, W. M. 2005, *MNRAS*, 210, 425
- Crutcher, R. M. 2004, *Ap&SS*, 292, 225
- Crutcher, R. M., Nutter, D. J., Ward-Thompson, D., & Kirk, J. M. 2004, *ApJ*, 600, 279

- Girart, J. M., Crutcher, R. M., & Rao, R. 1999, *ApJ*, 525, L109
- Goldreich, P., & Kylafis, N. D. 1981, *ApJ*, 243, L75
- . 1982, *ApJ*, 253, 606
- Lai, S., Crutcher, R. M., Girart, J. M., & Rao, R. 2002, *ApJ*, 566, 925
- Lai, S., Girart, J. M., & Crutcher, R. M. 2003, *ApJ*, 598, 392
- Lai, S. P. 1999, PhD thesis, University of Illinois at Urbana - Champaign, Urbana, IL 61801,
not Available at the Astronomy library at the Astronomy building
- Lazarian, A. 2003, *Journal of Quantitative Spectroscopy and Radiative Transfer*, 79, 881
- Liszt, H. S. 1995, *AJ*, 109, 1204
- Mezger, P. G., Zylka, R., & Wink, J. E. 1990, *A&A*, 228, 95
- Mooney, T., Sievers, A., Mezger, P. G., Solomon, P. M., Kreysa, E., Haslam, C. G. T., &
Lemke, R. 1995, *A&A*, 299, 869
- Motte, F., Schilke, P., & Lis, D. C. 2003, *ApJ*, 582, 277
- Rao, R., Crutcher, R. M., Plambeck, R. L., & Wright, M. C. H. 1998, *ApJ*, 502, L75+
- Sault, R. J., Teuben, P. J., & Wright, M. C. H. 1995, in *ASP Conf. Ser. 77: Astronomical
Data Analysis Software and Systems IV*, 433–+
- Vallée, J. P., & Bastien, P. 2000, *ApJ*, 530, 806

Table 1. Fractional polarization and Position angle for dust polarization observations at G30.79 FIR 10. Data was interpolated at a tolerance of $0.5''$ that corresponds to approximately 1.11×10^{-2} pc using a distance to G30.79 of 4.6 kpc.

Offsets in arcsec	P_{Dust}	ϕ_{Dust}
(-7.0,-9.0)	0.12 ± 0.05	62.3 ± 9.9
(0,-6.0)	0.09 ± 0.03	20.1 ± 8.3
(3.0,-2.0)	0.04 ± 0.009	24.8 ± 6.0
(0,-2.0)	0.023 ± 0.004	17.7 ± 5.0
(3.0,0)	0.03 ± 0.005	6.6 ± 5.3
(0,0)	0.02 ± 0.003	13.3 ± 4.3
(-2.5,0)	0.02 ± 0.005	11.5 ± 6.5
(3.0,3.0)	0.03 ± 0.004	-21.8 ± 4.6
(0,3.0)	0.01 ± 0.003	-6.6 ± 5.7
(3.0,6.0)	0.05 ± 0.01	-42.5 ± 6.8
(0,6.0)	0.03 ± 0.006	-24.3 ± 6.7

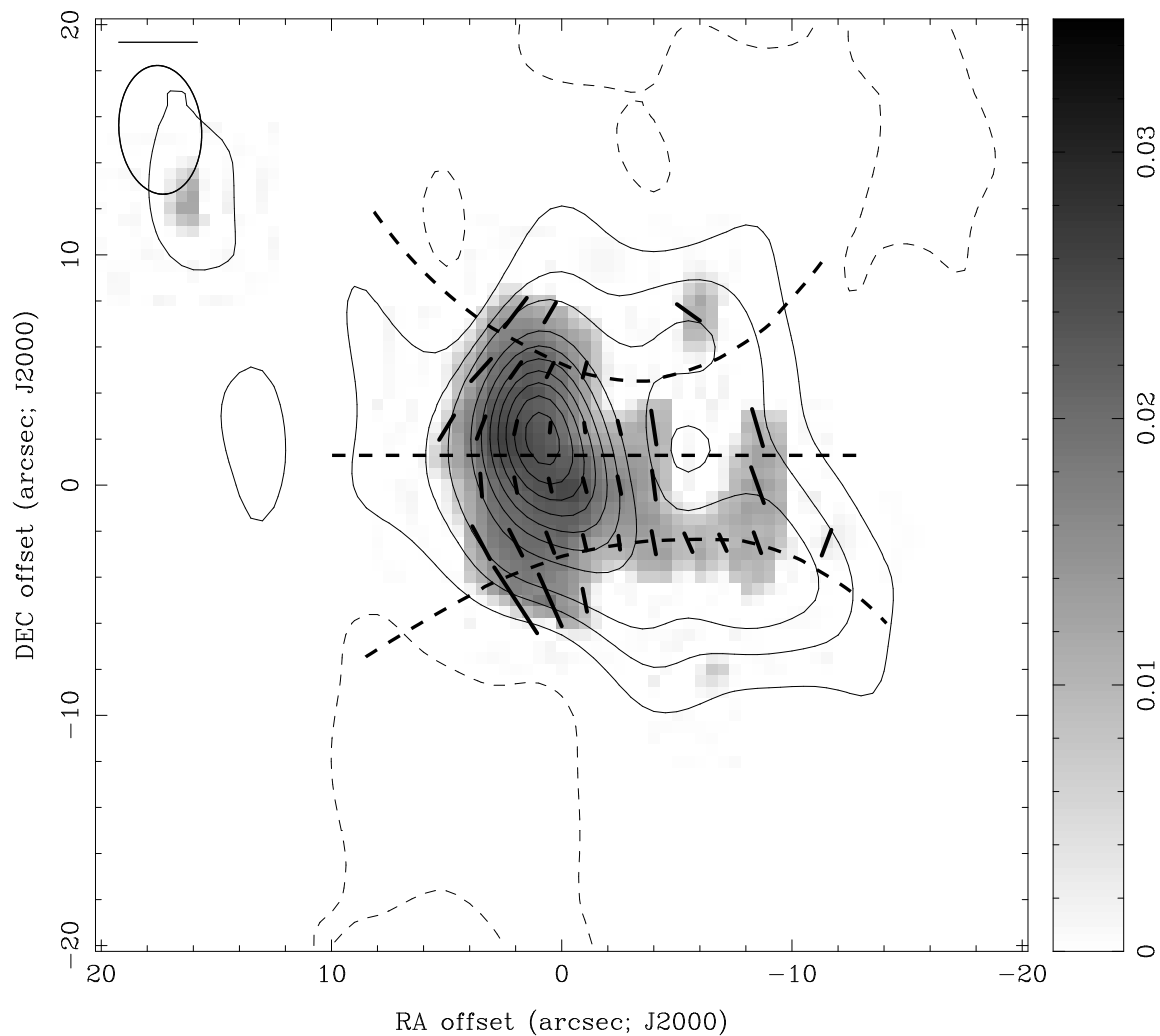


Fig. 1.— Polarization map of G30.79 FIR 10 at 1.3 mm. The contours represent the Stokes I emission at $-2, 2, 5, 8, 15, 20, 25, 30, 35, 40,$ and $45 \times \sigma$; $\sigma = 0.034$ Jy/beam. The pixel gray scale shows 3σ polarized intensity ($\sqrt{Q^2 + U^2}$) for the dust continuum emission, while the black line segments show the fractional polarization and P.A. The scale for the fractional polarization is given by the bar at the left corner that represents 0.1 fractional polarization. The thick dashed lines show the proposed magnetic field morphology.

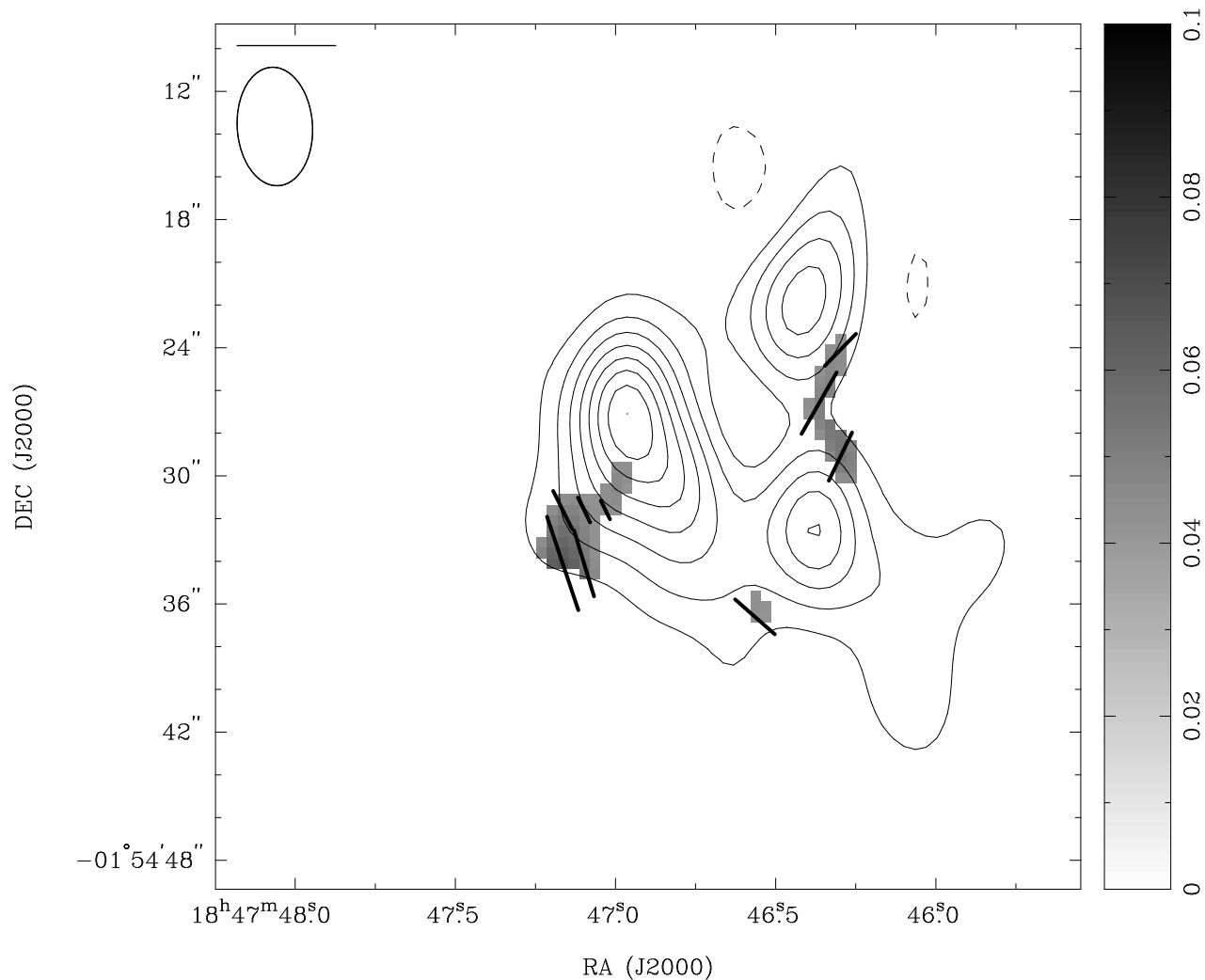


Fig. 2.— Polarization map of G30.79 FIR 10 for the CO $J = 2 \rightarrow 1$ line. The contours represent the Stokes I emission at -0.17, 0.17, 0.35, 0.52, 0.7, 0.88, 1.05, and 1.23 Jy/beam. The pixel gray scale shows 3σ polarized intensity ($\sqrt{Q^2 + U^2}$) for the CO $J = 2 \rightarrow 1$ emission, while the black line segments are the polarized line segment map for the CO $J = 2 \rightarrow 1$. The scale for the line segments is given by the bar at the left corner that represents 0.31 in fractional polarization.